NASA CONTRACTOR REPORT

Report No. 61306

PREDICTION OF GEOMAGNETIC ACTIVITY

By Kenneth Moe and Nancy U. Crooker

McDonnell Douglas Astronautics Co.
Western Division
Santa Monica, California 90406

August 1969

Prepared for

NASA-GEORGE C. MARSHALL SPACE FLIGHT CENTER
Marshall Space Flight Center, Alabama 35812

TECHNICAL REPORT STANDARD TITLE PAGE

1. REPORT NO.	2. GOVERNMENT ACCESSION NO.	3. RECIPIENT'S CATALOG NO.
NASA CR-61306		

4. TITLE AND SUBTITLE	5. REPORT DATE
PREDICTION OF GEOMAGNETIC ACTIVITY	August 1969
	6. PERFORMING ORGANIZATION CODE
7. AUTHOR(S)	8. PERFORMING ORGANIZATION REPORT #
Kenneth Moe and Nancy U. Crooker	
9. PERFORMING ORGANIZATION NAME AND ADDRESS	10. WORK UNIT NO.
McDonnell Douglas Astronautics Co./Western Division Santa Monica, California 90406	11. CONTRACT OR GRANT NO. NAS8-30156
	13. TYPE OF REPORT & PERIOD COVERED Contractor Report
12. SPONSORING AGENCY NAME AND ADDRESS NASA-George C. Marshall Space Flight Center Marshall Space Flight Center, Alabama 35812	14. SPONSORING AGENCY CODE

15. SUPPLEMENTARY NOTES

Distribution of this report is provided in the interest of information exchange. Responsibility for the contents resides in the author or organization that prepared it.

16. ABSTRACT

Although several theories have been proposed, we still do not understand solar flares, nor do we understand how the solar energy propagates into the Earth's magnetosphere. Because of ignorance of the physical mechanisms, attempts to develop methods of predicting geomagnetic disturbances have usually involved correlation studies employing some of the phenomena associated with solar flares and geomagnetic storms. It has been known for decades that some geomagnetic storms occur several days after large solar flares, but that in other cases storms will recur for several solar rotations without the recurrence of major flares. The unequivocal separation of flare-associated storms from recurring storms first became possible with the launching of the Mariner space probes. The first probe which has been in a convenient position for predicting recurring storms is Pioneer 7. Even with Pioneer 7, however, serious predictive problems remain because the energy spectra of solar emissions can vary greatly from storm to storm, and not all precursors are invariably present. In this report, the predictive capability of several newly available tools is evaluated: the study of the solar wind speed by Neugebauer and Snyder, the study of PCA spectra by Castelli et al., the study of energetic electrons by Anderson and Lin, the study of the interplanetary field direction by Fairfield, and the study of the perpendicular fluctuations of the interplanetary field by Balliff et al. These measurements are introduced into a mathematical formulation to predict the contributions to geomagnetic disturbance of persistent streams and flare-associated streams of solar plasma. Simulated numerical predictions of A_p using various combinations of the precursors are compared with the measured values of A_p.

17. KEY WORDS	18. DISTRIBUTION STATEMENT
	PUBLIC RELEASE E. D. Geissler E. D. GEISSLER, Director Aero-Astrodynamics Lab, MSFC

19. SECURITY CLASSIF. (of this report)	20. SECURITY CLASSIF. (of this page)	21. NO. OF PAGES	22. PRICE
U	U	43	

MSFC - Form 3292 (May 1969)

FOREWORD

This work was conducted under the sponsorship of the Aerospace Environment Division, Aero-Astrodynamics Laboratory, NASA-Marshall Space Flight Center. The technical monitor of this contract was Dr. L. L. DeVries. This effort represents part of the continuing study to develop a better understanding of relationships between the solar and terrestrial environment to furnish improved space environment criteria and operational support for present and future space programs.

TABLE OF CONTENTS

LIST OF FIGURES

LIST OF TABLES

Section 1

INTRODUCTION

During geomagnetic storms, the air drag on artificial satellites increases, and radio and radar transmissions at high latitudes are impaired. There have been many attempts to develop reliable techniques of predicting magnetic storms in order to improve satellite orbital predictions and arctic radio propagation; but none of these attempts has been completely successful, for several reasons:

1. None of the precursors is wholly reliable.

2. Some of the precursors are monitored for only a fraction of the day.

3. Until the launching of Pioneer VII, there was no practical way of monitoring the long-lived tongues of enhanced plasma which apparently cause the recurring type of geomagnetic storm.

The study described in the present report utilized Pioneer VII data and several other precursors in an attempt to overcome the limitations enumerated above. The report begins with a section on the meaning and uses of K_p and A_p. The kinds of data considered for use in short-term predictions of K_p are then described and evaluated. The prediction equations are next explained, and a detailed numerical example is given. A graphical presentation of the predictions follows. The errors in these simulated predictions are discussed and mathematically analyzed. Suggestions are made for future research on short-term predictions. Long-term predictions of the annual average of $\overline{A_p}$ are then presented, and their errors are estimated. The main results of this study are summarized at the end of the report.

Section 2

THE MEANING AND USES OF K_p AND A_p

The geomagnetic index K_p and the geomagnetic planetary amplitude A_p are measures of the level of geomagnetic disturbance. Specifically, A_p is a daily average of the eight three-hourly ranges of disturbance at stations just equatorward of the auroral zone, while K_p is a quasi-logarithmic function of the ranges of disturbance (Reference 1). Although A_p is called a planetary index, it is not proportional to the range of disturbance at any latitude except near 57°, where it is measured. At most other latitudes, the range is nearly proportional to K_p at low levels of disturbance, and nearly proportional to A_p at high levels of disturbance (Reference 2). The relationships among K_p, A_p, the sum of the eight three-hourly values of K_p (ΣK_p), and the range at the peak of the auroral zone are given in Table 1.

K_p and A_p are important because they provide quantitative measures of geomagnetic disturbance. During magnetic storms, radio and radar propagation are disturbed, particularly at high latitudes. The air drag on artificial satellites also increases, causing errors in the predicted ephemerides. If K_p and A_p could be accurately predicted, radio propagation and orbital prediction could be improved. This is the motivation of the present study.

Because of the importance to the Marshall Space Flight Center of the relationship between geomagnetic storms and atmospheric density, the following information on the "corpuscular heating effect" is reproduced from Reference 3:

> During geomagnetic disturbances, the atmospheric density at satellite altitudes increases. This increase is usually represented as an equivalent increase in the exospheric temperature of an atmospheric model. The phenomenon is therefore called "the Corpuscular Heating Effect," even though the physical processes involved and the existence of a temperature increase at low latitudes have not been established by direct measurements. The corpuscular heating effect is a highly nonlinear function of the geomagnetic planetary amplitude, A_p, as is shown by the three curves in fig. 1, which

TABLE 1

RELATIONSHIPS AMONG MEASURES OF GEOMAGNETIC DISTURBANCE

Ap (2 gammas)	Kp	$\sum$ Kp	Daily Range At Peak of Auroral Zone (Relative Units)
0	0 o	0	0
2	0 +	2.7	.031
3	1 -	5.3	
4	1 o	8.0	
5	1 +	10.7	.08
6	2 -	13.3	
7	2 o	16.0	
9	2 +	18.7	.158
12	3 -	21.3	
15	3 o	24.0	
18	3 +	26.7	
22	4 -	29.3	.334
27	4 o	32.0	
32	4 +	34.7	
39	5 -	37.3	
48	5 o	40.0	.40
56	5 +	42.7	
67	6 -	45.3	.54
80	6 o	48.0	.66
94	6 +	50.7	
111	7 -	53.3	
132	7 o	56.0	
154	7 +	58.7	.80
179	8 -	61.3	
207	8 o	64.0	1.03
236	8 +	66.7	
300	9 -	69.2	(1.48⁻)
400	9 o	72.0	(1.96)

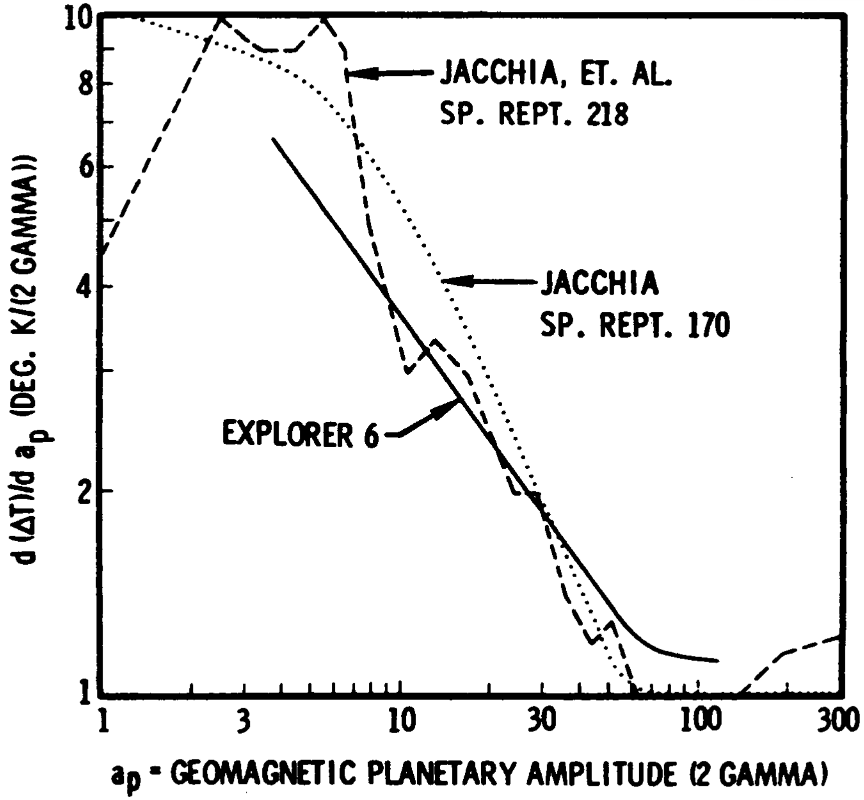

Figure 1. Derivative of Corpuscular Heating from Satellite Drag at Low Latitudes

give the increment in exospheric temperature corresponding to a unit increase in A_p. These curves are based on satellite drag measurements at low and middle latitudes (Reference 4). The corpuscular heating effect is much larger at high latitudes (Reference 5), where the dependence on A_p has been reported to be somewhat different than at lower latitudes, but still highly nonlinear (References 6, 7). These nonlinear relationships were unexpected, and require an explanation.

The investigation of the nonlinear relationships was begun by examining the geomagnetic disturbance currents as a function of A_p and latitude. The latitude dependence is illustrated for low and high levels of disturbance in figs. 2 and 3, respectively, (Reference 2). The spreading of the disturbed auroral region to lower latitudes during storms can be clearly seen.

The ranges at several locations have been normalized and plotted against A_p in fig. 4. K_p has also been plotted against A_p, using the right-hand scale. The locations are the trough near 20°, the average latitude of stations used to construct K_p and A_p (57°), the peak of the disturbed region around the auroral zone, and the polar cap (80°). The normalized range at 57° differs from the normalized curve for A_p by no more than 30%. At all other latitudes disturbance varies more like K_p than A_p at the low values, but more like A_p at the high values. This behavior is qualitatively the same as that of the three curves in fig. 1. At this point we should mention that Truttse (Reference 8) has recently shown that the density perturbations at low and middle latitudes during geomagnetic storms are linearly related to the AE index averaged over the preceding 10 hours. This would be approximately proportional to the height of the peak, because the AE index is a measure of auroral electrojet activity.

The two principal theories which have been proposed to explain the corpuscular heating effect are Dessler's (Reference 9) and Cole's (Reference 10). Dessler suggested that this effect is caused by the absorption of

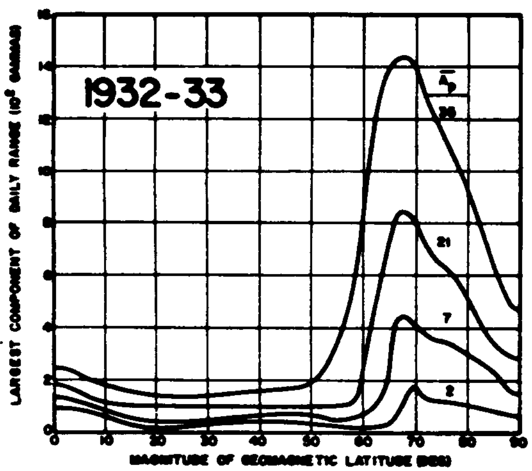

Figure 2. Largest Component of Daily Range Versus Geomagnetic Latitude (1932 – '33)

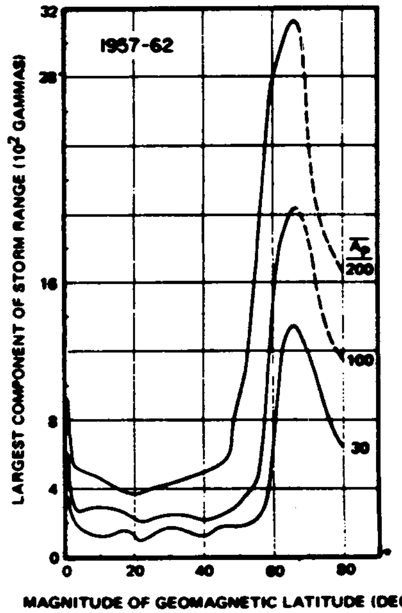

Figure 3. Largest Component of Storm Range Versus Geomagnetic Latitude (1957 – '62)

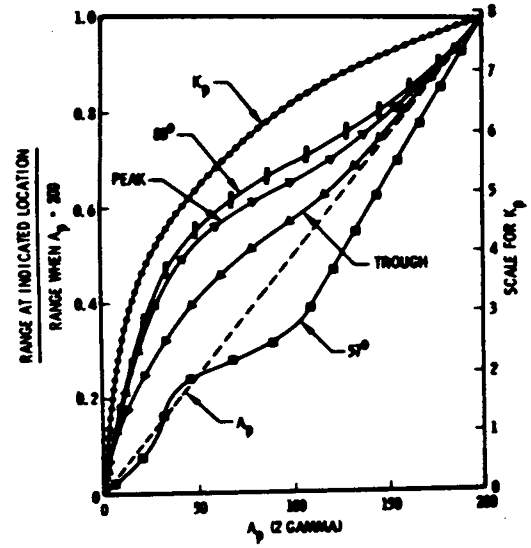

Figure 4. Normalized Ranges at Various Locations vs Ap and Kp

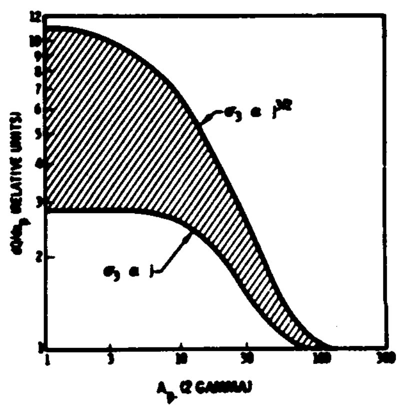

Figure 5. Derivative of Corpuscular Power Input from Storm Ranges at High Latitudes

magnetohydrodynamic waves in the ionosphere. Dessler's theory has now been disproved by Campbell (Reference 11). Cole applied to the ionosphere earlier work by Cowling and by Piddington on electric fields and forces in plasmas of astrophysical interest. Cole showed that the power input Q to unit volume of the high-latitude ionosphere caused by disturbance currents J is $Q = j^2/\sigma_3$, where σ_3 is the Cowling conductivity. σ_3 increases during geomagnetic disturbances, but the functional relationship is unknown. A method of estimating the dependence of σ_3 on j will now be described.

As Dessler has pointed out, nearly all of the geomagnetic disturbance at low and middle latitudes is caused by the ring current, which cannot directly heat the atmosphere. The corpuscular energy input must therefore occur in the auroral zones and polar caps. The mechanisms which might transfer part of this effect to the lower latitudes are mass outflow caused by a pressure gradient (Reference 10), and the dissipation of the energy of large traveling ionospheric disturbances (Reference 12) by the type of viscous interaction which Hines has often described (Reference 13). Neither of these ideas for explaining the observed effects at low and middle latitudes has been subjected to quantitative calculation, but if one assumes that the fraction of the corpuscular energy (deposited at high latitudes) which is transported to the lower latitudes is independent of A_p, then the dependence of σ_3 on j can be calculated.

The disturbance currents represented by the perturbations of the geomagnetic field in figs. 2 and 3 have been integrated over the auroral zone and polar cap. The resulting total current has been inserted in Cole's equation to calculate Q under two different assumptions, $\sigma_3 \propto j$, and $\sigma_3 \propto j^{3/2}$. The normalized results are shown in fig. 5, with the area shaded between the curves representing the two cases. Notice that the experimental data in fig. 1 would fit between these two curves, implying that the Cowling conductivity increases slightly faster than the ionospheric currents.

In support of this idea, we note that Wescott et al. (Reference 14) have observed in a number of barium-cloud experiments in the auroral zone that the electric field is anticorrelated with aurora. Of course, we have been relating the energy deposited in one cubic centimeter of the auroral zone to the exospheric temperature rise of a vertical column at low and middle latitudes, so the calculation is far from exact. The important point is that the highly nonlinear relationship between A_p and the temperature increase is capable of being explained in terms of the corpuscular energy input at high latitudes and its transmission to low latitudes. It is essential for the construction of realistic global atmospheric models that the corpuscular heating effect be correctly described. Detailed calculations should be carried out employing the theoretical ideas of Cole and Hines. Despite the poor spatial resolution of the polar satellite data, DeVries et al. (Reference 15) have been able to show by means of a multiple-correlation analysis that the time delay in the response of the atmosphere to the corpuscular energy source is proportional to the distance between the auroral zone and the perigee point, thus verifying that the energy is first deposited at high latitudes, and then is transported to low latitudes. Now that accelerometers and pressure gauges have been placed in polar orbits, better measurements of the latitude dependence of the corpuscular heating effect are becoming available. This will enable the theories to be tested and the corpuscular heating process to be better understood.

Improved atmospheric models can then be constructed. The prediction of values of K_p or A_p to insert into these models is the subject of the present report.

Section 3

SHORT TERM PREDICTIONS OF ΣK_p

This section describes the equations and the kinds of measurements which were used in predicting ΣK_p and compares these simulated predictions with the measured values of ΣK_p.

3.1 DATA

The following data were considered for use in the prediction formula for ΣK_p:

1. Solar wind speed
2. 10 cm solar radio noise bursts
3. Sudden ionospheric disturbances
4. Outstanding x-ray events
5. PCA events
6. Solar flares
7. Interplanetary field variations
8. Electron events
9. Sunspot areas in equatorial zone of sun
10. Neutron-monitor measurements
11. Magnetic crochets

Data items 1, 5, 7 and 9 were chosen because they had previously been individually correlated with K_p or A_p by Snyder et al. (Reference 16), Moe (Reference 17), Coleman et al. (Reference 18) and Gnevyshev (Reference 19), respectively. The remaining items are all associated with geomagnetic activity and were thought to be readily available. The first five data items are used in the final prediction formula and will be discussed in the following section. The last six were rejected for a variety of reasons: The solar flare data, published in Solar-Geophysical Data (Reference 20) were found to be too qualitative, incomplete, and unwieldy for the present purposes. Ballif et al. (Reference 21) found that the correlation between K_p and interplanetary field variations is greatly reduced when the satellite taking the measurements is more than a few degrees of heliocentric angle from the earth. Thus, such data would probably not be useful for two-day predictions. The prompt fluxes of electrons with energies greater than 40 Kev from solar flare electron events, obtained from Anderson (Reference 22 and unpublished data), were compared with K_p. There was a good correlation with K_p two or three days later. Prompt electron data were not used in the simulated predictions because they are not yet available for 1968; however, if they were available in real time, they would be useful for predictions. Gnevyshev (Reference 19) shows a long-term correlation between A_p and sunspot areas in the equatorial region of the sun. However, analysis of 300 sunspot photographs supplied by Lt. Isbelle of the USAF Solar Observatory at Van Norman Reservoir (near Los Angeles) did not reveal any significant day-to-day or month-to-month correlation. Data items 10 and 11 were not used because of incompleteness.

3.2 REDUCTION OF DATA

The prediction formula,

$$K(t) = K_M(t) + K_F(t) \quad , \tag{1}$$

where K is the predicted value of ΣK_p, reflects two apparent contributions to the geomagnetic index; K_M is the contribution due to long-lived, active regions on the sun, and K_F is that due to flare-associated burst phenomena.

The basic data to be used in the prediction formula are the solar wind speed measurements made by the Pioneer VII satellite. This data has been published in Solar-Geophysical Data since December of 1967. Pioneer VII orbits the sun in a position such that it sees a particular meridian of the sun τ days sooner than the solar rotation causes the earth to see this same meridian (see Figure 6). Hence, first-order predictions, using only solar wind speed data, can be made τ days in advance. Snyder et al. (1963) showed a good correlation between ΣK_p and the solar wind speed U from Mariner IV data according to the formula

$$U = 8.4\Sigma K_p + 330 \text{ km/sec}$$

(See Figure 7.)

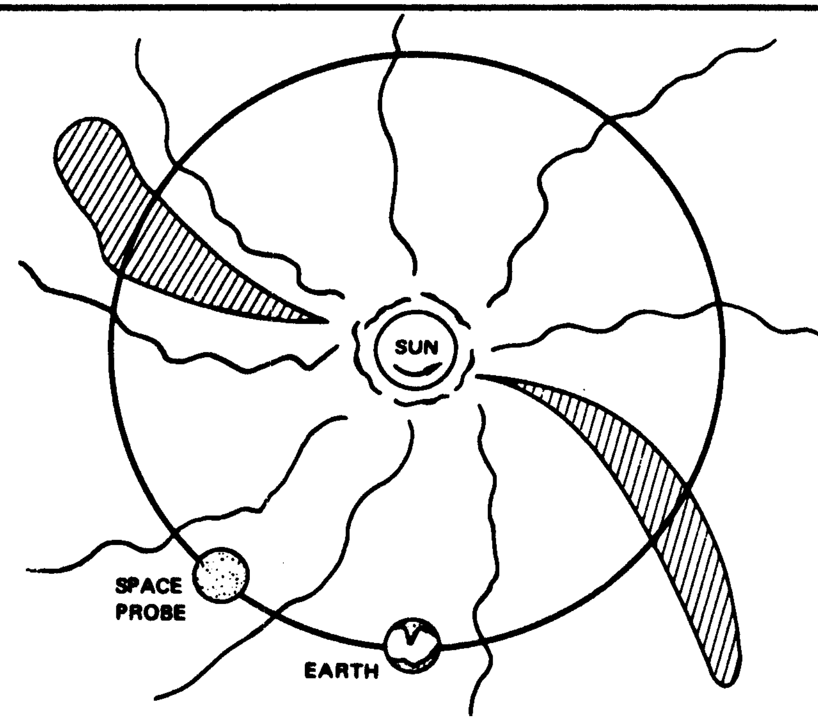

Figure 6. Pioneer 7 Space Probe following Earth in Orbit about the Sun. Because of the Solar Rotation, the long-lived tongues of enhanced solar plasma sweep over the Space Probe 2 days before they sweep over the Earth. In the present study, the Solar-wind speed measured by Pioneer 7 is used to predict the contribution to Geomagnetic disturbance made by these long-lived Plasma Tongues.

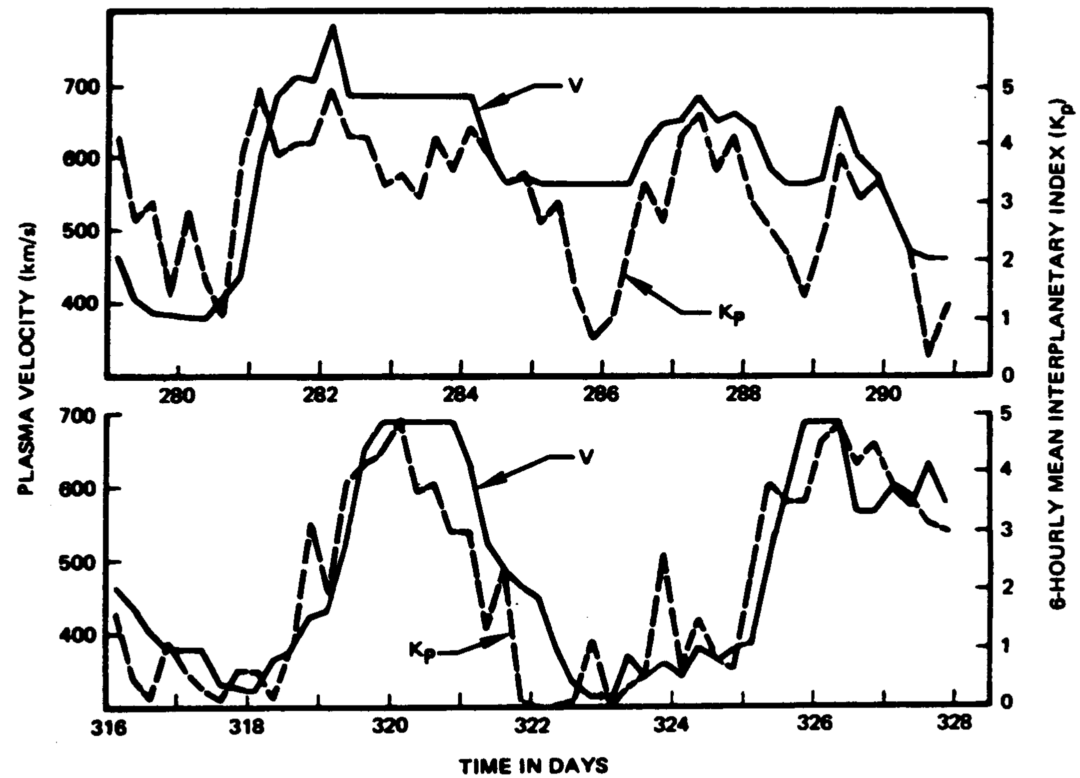

Figure 7. Comparison of Solar-Wind Speed with K_p (After Snyder, et al)

In the present study the preliminary formula, patterned after that of Snyder et al., is

$$U = 10 K' + 300 \text{ km/sec} \tag{2}$$

where K' is the preliminary prediction of ΣK_p and U is the solar wind speed as measured by Pioneer VII. In applying Equation 2, the U data must be co-rotated such that U on a certain day predicts ΣK_p at the earth τ days later.

If τ were equal to zero, there would be no need to separate the active region and flare-associated contributions to ΣK_p, since U is assumed to reflect all magnetic activity. Of course, in this case, Equation 2 would no longer be a prediction. Because τ is on the order of days, however, the prediction formula may be improved by considering the two contributions separately; the flare-associated contributions to ΣK_p from a particular event must be added to K' at the time of the event, since the data were taken τ days before the event, and subtracted from it τ days later.

Thus, the final prediction formula in terms of K' is

$$K(t) = [K'(t-\tau) - K_{FS}(t-\tau)] + K_F(t) \quad , \tag{3}$$

where the bracketed term represents $K_M(t)$ and K_{FS} represents flare-associated contributions at the satellite. Implicit in Equation 3 is the assumption that the flare-associated events recorded at the earth affect both the satellite and the earth in the same manner. This assumption will be made obvious in the more detailed discussion to follow.

The flare-associated events used as precursors of geomagnetic activity in the present prediction scheme are items 2-5 listed in Section 3.1. The 10 cm solar radio flux measurements are obtained from the Sagamore Hill Observatory of the Air Force Cambridge Research Laboratories. These data are taken continuously during daylight hours. The sum of the mean flux densities of each day's bursts is the parameter used in the predictions. Of the sudden ionospheric disturbances, the sudden phase anomalies are the chosen parameter because of the worldwide distribution of SPA observations. These data are published in Solar-Geophysical Data. The reported degrees of phase shift are all assigned a positive sign and then summed for each day. The outstanding x-ray events, published in the same bulletin, are measured by satellite. The 1A to 20A fluxes are summed for each day. The polar cap absorption (PCA) events are recorded at the McDonnell Douglas Astronautics Company's geophysical observatories in the Arctic and Antarctic.

To obtain $K_{FS}(t - \tau)$ and $K_F(t)$ from the precursor data, three scaling functions are used. The first function, shown in Figure 8, is the expected relative contribution to ΣK_p as a function of the longitude of the flare associated with a particular precursor. This curve is based on Akasofu's (Reference 22) correlations between the amplitudes of several storm characteristics and associated flare longitudes. Accordingly, for the precursor data for which associated flare longitudes are known, the raw data is reduced by the appropriate factor. Flare longitudes are usually known for most of the PCA events and sudden phase anomalies. In the course of making simulated predictions, however, it was decided that the effect of taking flare longitude into account for sudden phase anomalies is negligible.

The second function, shown in Figure 9, is the expected relative contribution to ΣK_p as a function of the time of the precursor (or the associated flare, since the time delay between the two is negligible for the present study). This curve is based on the general knowledge that a geomagnetic storm will peak at approximately two and a half days after the occurrence of the associated flare. All of the precursor data is thus further reduced by the appropriate time delay factor.

The third function, shown in Figure 10, is used to convert the reduced precursor data to ΣK_p units. The curve is based on an experimental relationship between

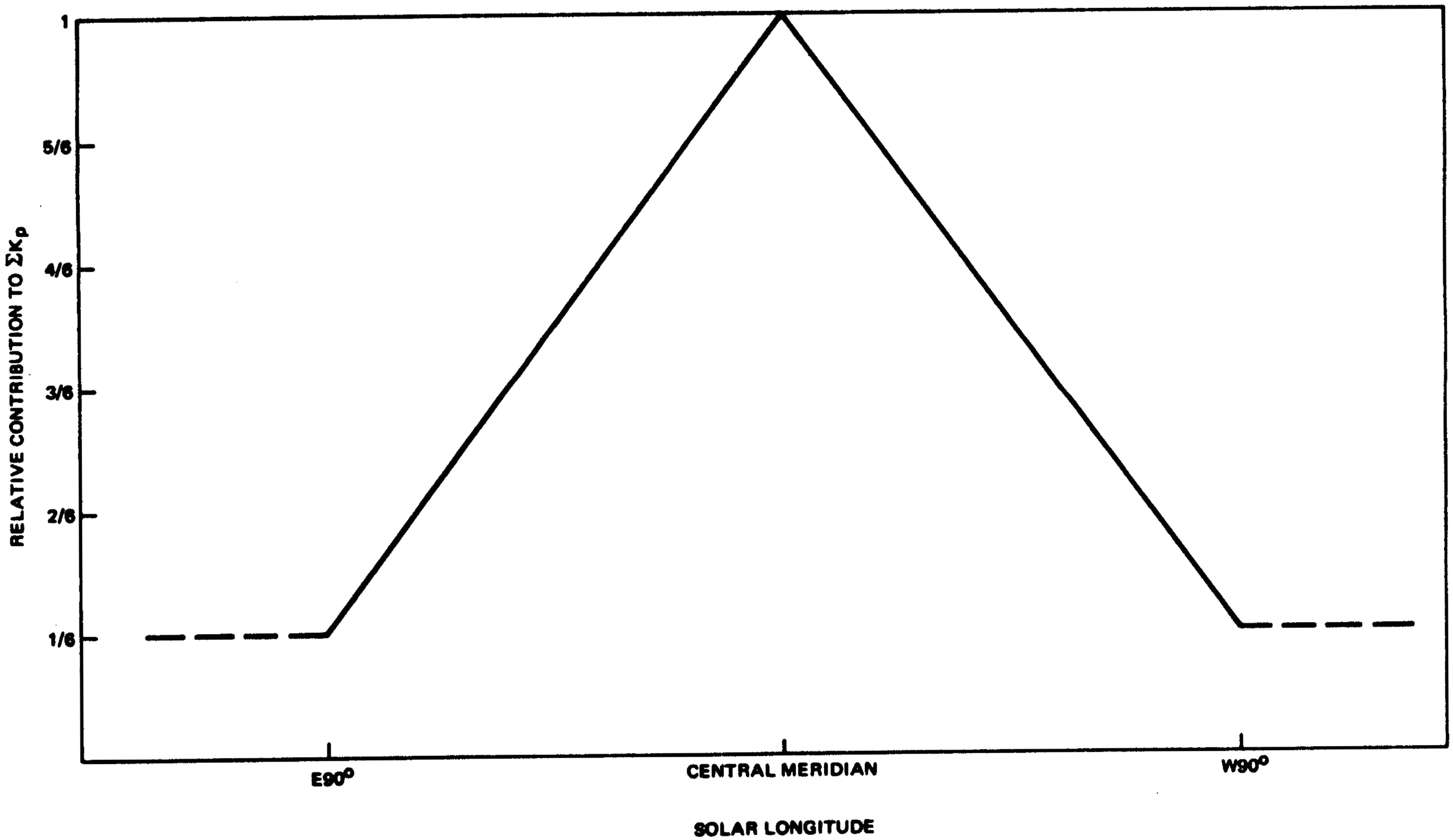

Figure 8. Relative Contribution to ΣK_p vs Solar Longitude of Flare

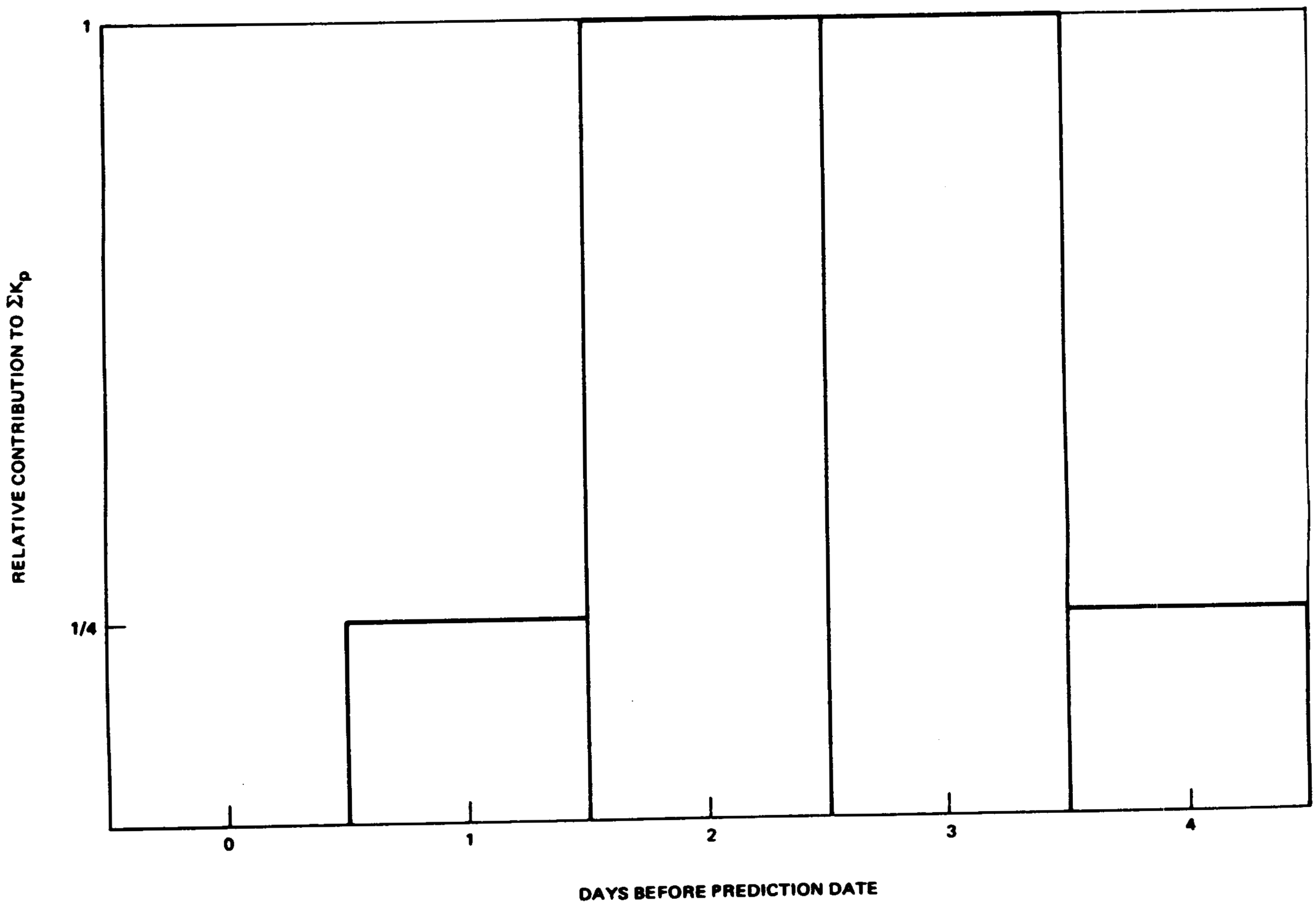

Figure 9. Relative Contribution to ΣK_p vs Days before Prediction Date of Precursor Events.

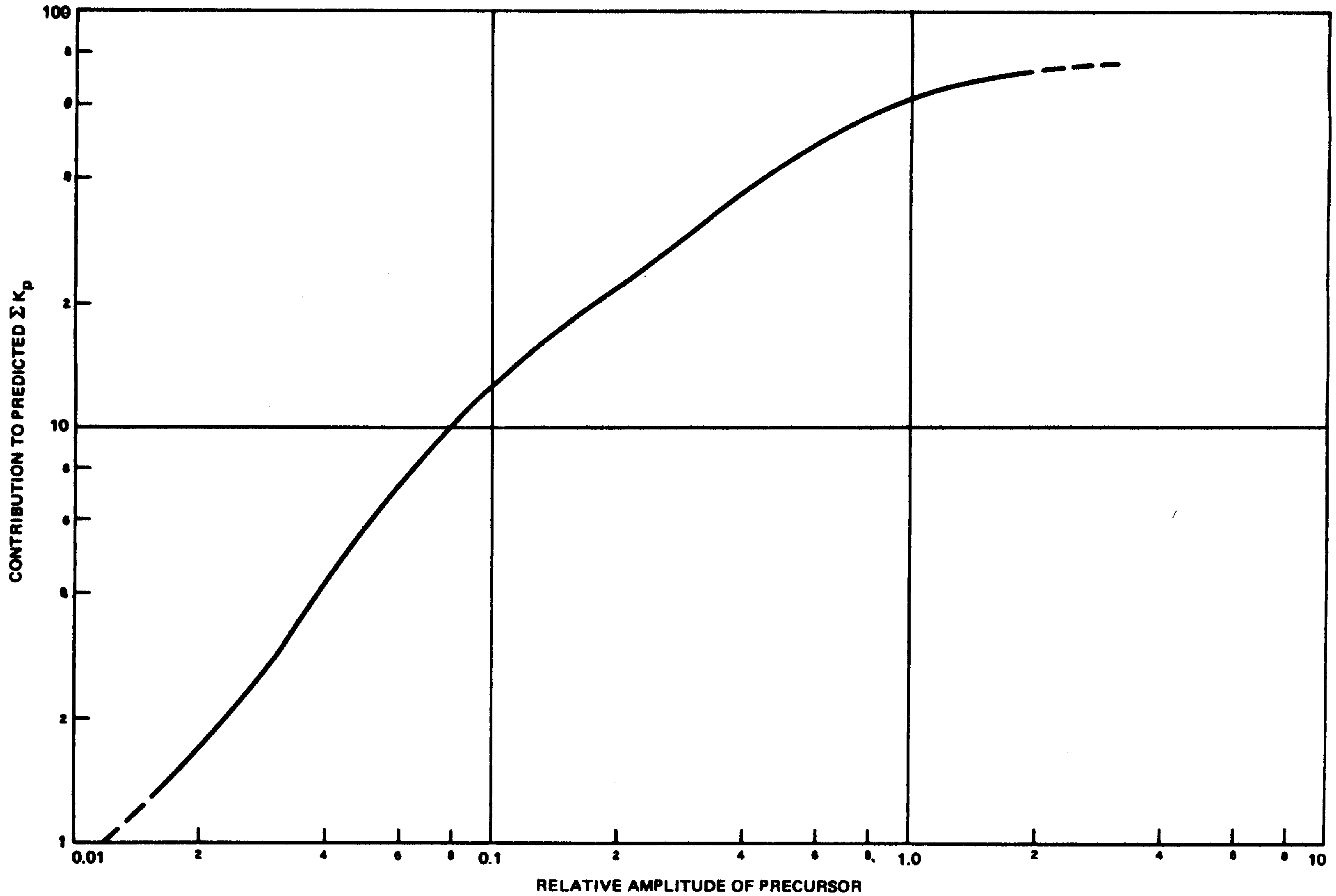

Figure 10. Contribution to Predicted ΣK_p vs Relative Units of Reduced Amplitude of Precursor

ΣK_p and the range of geomagnetic disturbance at the peak of the auroral zone, converted to relative units (based on Reference 2). To decide how many of each of the precursors' units correspond to 1.0 relative units on the abscissa of this curve, the factors yielding the best prediction for nine assorted days in 1968 were chosen. An attempt was made to give equal weight to each of the four precursors. Table 2 lists the chosen conversion factors. When the contribution to ΣK_p for a particular event was less than 1.0, the curve was linearly extrapolated on the logarithmic graph.

TABLE 2

FACTORS USED TO CONVERT VARIOUS PRECURSOR UNITS TO ΣK_p UNITS

PRECURSOR	NUMBER OF UNITS EQUAL TO 1.0 RELATIVE UNIT ON ABSCISSA OF GRAPH IN FIGURE 10
10 cm solar radio flux	10^{-18} watts m^{-2} H_z^{-1}
Sudden phase anomalies	100,000 degrees
Outstanding x-ray events	10 (0-8A) } emissivities
	100 (8-20A) } emissivities
PCA events	100 decibels

To exemplify the above procedure, a simulated prediction for June 16, 1968, follows. At this time, τ was equal to 5 days. The solar wind speed U on June 11 was 525 km/sec. Substituting this value into Equation 2 yields the initial prediction K',

$$K' = 1/10\ (525 - 300) = 22.5$$

To calculate K_{FS}, account is taken of all precursor events which occurred from one to four days before June 11, and each event is multiplied by the appropriate scaling factors. For example, a PCA event of amplitude 5.7 db associated with a flare located at 8°W on the sun's disk relative to the earth, occurred on June 9. The value of 5.7 db is first multiplied by 1/3 for flare longitude, according to Figure 7, taking into account that the satellite is 70° east of the earth, relative to the sun.

$$\left(\frac{\tau}{\text{sun's period}}\,360^\circ = \frac{5}{27.5}\,360^\circ = 70^\circ \quad .\right)$$

The resultant value of 1.9 db is then multiplied by 1 for storm time delay, according to Figure 8, and by 1/(100 db), according to Table 2. This yields a relative value of 0.019, which corresponds to 1.6 ΣK_p units on the graph in Figure 9. Similar calculations for all other precursors which occurred one to four days before June 12 are listed in Table 3. For these remaining precursors, longitude of the associated flare was not taken into account.

TABLE 3

SAMPLE PREDICTION CALCULATION

PRECURSOR	DATE	AMPLITUDE ×	TIME DELAY FACTOR ×	$\frac{1}{\text{TABLE 2 FACTOR}}$	=X	X IN K_p UNITS
10 cm flux	6-9	2.06×10^{-21}	1	10^{18}	.00206	.1
Sudden phase anomalies	6-7	253	¼	10^{-5}	.00063	.1, negligible
"	6-8	290	1	10^{-5}	.00290	.2
"	6-9	805	1	10^{-5}	.00805	.8
"	6-10	100	¼	10^{-5}	.00025	.1, negligible
X-ray event (0-8A)	6-7	1.47×10^{-2}	¼	10^{-1}	.00037	.1, negligible
(8-20A)	6-7	1.08×10^{-1}	¼	10^{-2}	.00027	.1, negligible
(0-8A)	6-9	2.89×10^{-2}	1	10^{-1}	.00289	.2
(8-20A)	6-9	2.20×10^{-1}	1	10^{-2}	.00220	.2

Summing the results of the above calculations, including the PCA contribution, yields $K_{FS} = 3.1$. The remaining parameter in Equation 3, K_F, is calculated in a comparable manner for all precursors occurring two to four days before June 16. (Because the prediction is for two days in advance, those precursors occurring one day before June 16 cannot be taken into account. However, the amount contributed to the ΣK_p one day before the fact is usually negligible.) During this time interval, the only activity which occurred were sudden phase anomalies on June 13 of total amplitude 120°, yielding a contribution of 0.1 to K_F. The two-day prediction K is obtained by substituting K', K_{FS} and K_F into Equation 3; the result is

$$K = K' + K_F - K_{FS} = 22.5 + 0.1 - 3.1 = 19.5 \quad .$$

The actual value of ΣK_p for June 16 was 18.

3.3 DISCUSSION OF RESULTS

Simulated predictions of ΣK_p for 1968 made by the above method are compared with the actual values of ΣK_p in Figure 11. The solid line represents ΣK_p. The dashed line represents predictions based on the co-rotated Pioneer VII solar wind measurements alone. The dotted line represents predictions based on both solar wind measurements and flare-associated events, using Equation 3. A solid triangle is placed on the time scale every 27 days, but there is not much evidence of 27-day recurrence in these data. To investigate this question further, 27-day differences in ΣK_p were calculated. They were larger than 5 units most of the time, often much larger. This again indicates little recurrence tendency. It is expected that a 27-day recurrence tendency will be more prominent after sunspot maximum.

There is little difference between the dashed and dotted lines in Figure 11, except near the beginning of November. This means that flare-associated events made a negligible contribution to the computed ΣK_p, except during November. On the other hand, the lack of a clear 27-day recurrence tendency indicates that the plasma tongues are rapidly evolving, and causes one to

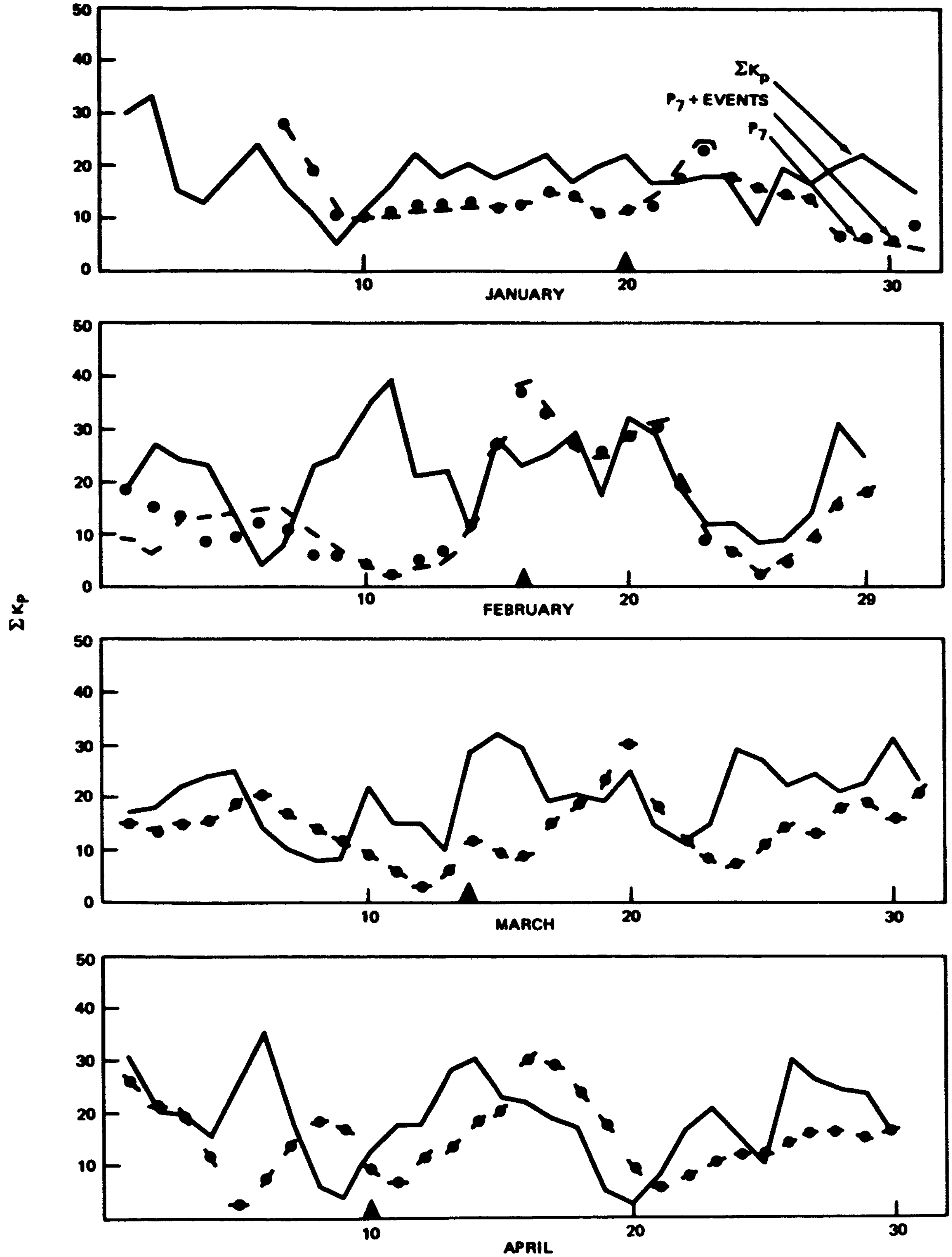

Figure 11a. Comparison of Predicted and Actual ΣK_p

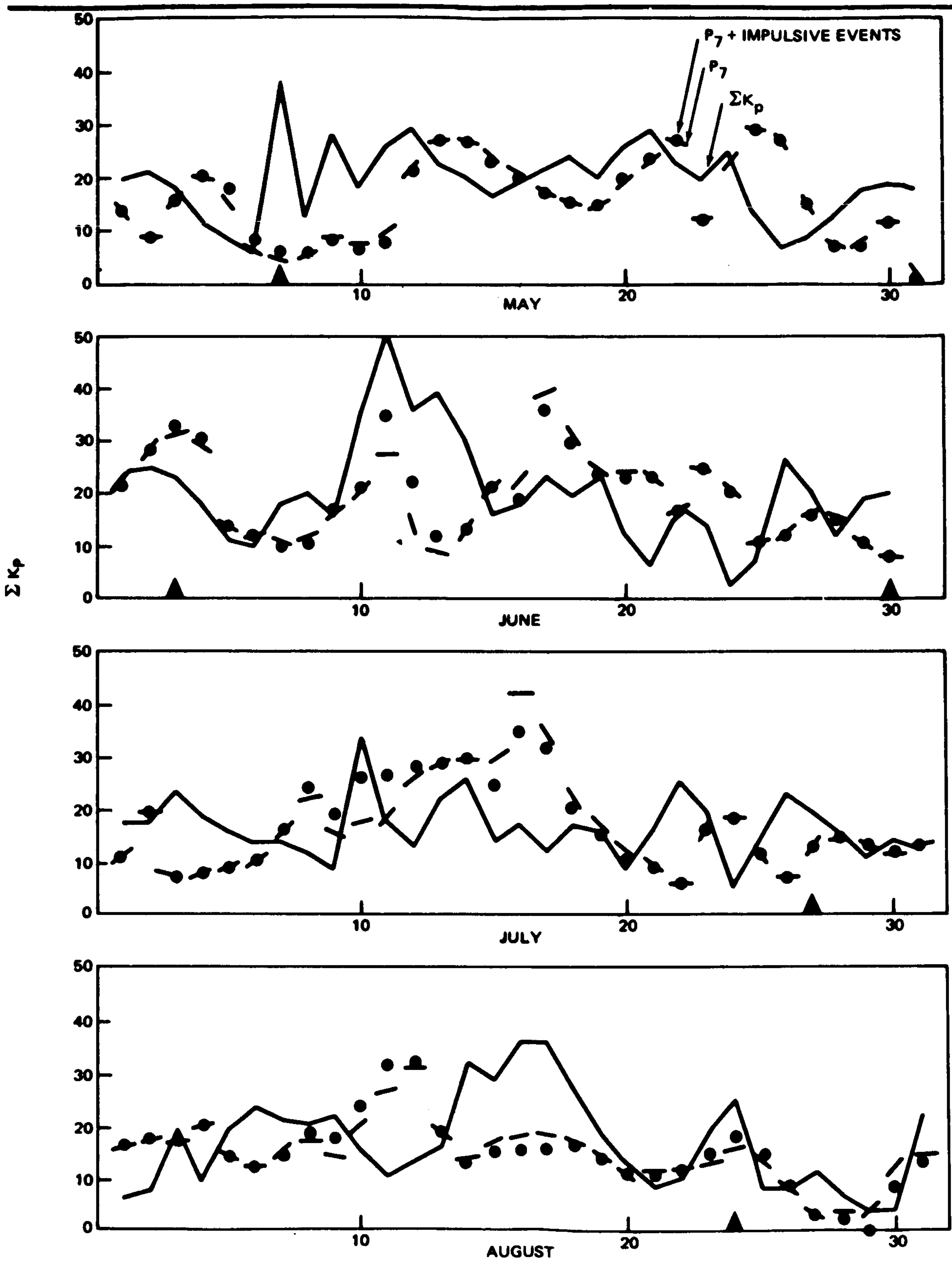

Figure 11b.

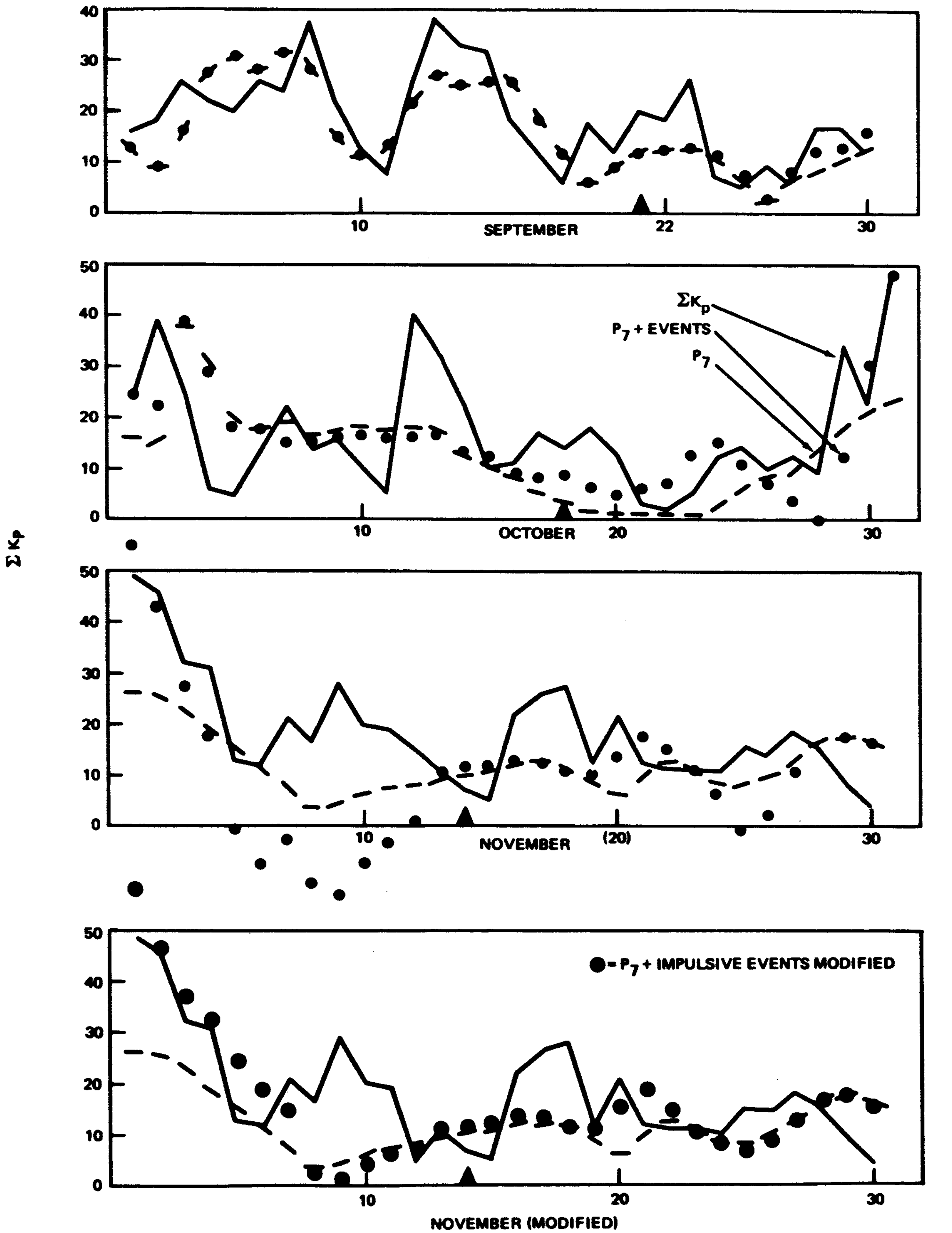

Σ Kp
40
30
20
10
0
10
SEPTEMBER
22
30
50
40
30
20
10
0
ΣKp
P7 + EVENTS
P7
10
OCTOBER
20
30
50
40
30
20
10
0
10
NOVEMBER
(20)
30
50
40
30
20
10
0
● = P7 + IMPULSIVE EVENTS MODIFIED
10
20
30
NOVEMBER (MODIFIED)

Figure 11c

expect flare-associated events to be more important.

Because of the large flare-associated events at the beginning of November, large adjustments were made in the solar wind speed. Apparently there was an overcorrection, because the prediction ΣK_p sometimes went negative. An alternative dependence of flare-associated emissions on the angular distance from central meridian passage has also been used in Figure 11C to obtain a revised prediction for November which does not go negative. There were no other large events in 1968, so this revised angular dependence could not be tested on independent data.

Some of the smaller geomagnetic storms which appear not to be flare-associated may actually be associated with flares which did not produce enough penetrating solar radiation to affect riometers (~ 0.5 db), yet might have been observable with ionosondes at polar stations (Reference 24), or by forward scatter (Reference 25). A search for small PCA's, using ionosonde and forward scatter data for 1968, would be desirable when such data become available. In an earlier study (Reference 17), it was shown that some of the smaller storms during the first six months of the IGY were preceded by PCA's which were detected by ionosondes, but not by riometers.

A number of statistical tests have been performed on the data and the predictions. The first group of tests was intended to evaluate the rate of evolution of the plasma tongues and the ease with which their effects penetrate into the earth's magnetosphere. As part of these tests, it was necessary to estimate the effects of biases and random errors of measurement on the reported values of solar wind speed. The results of these tests are represented as standard deviations in Table 4.

TABLE 4

STANDARD DEVIATIONS OF PLASMA SPEED MEASUREMENTS

Quantities	P7(t) - P7(t + 27)	P7(t) - P7(t + 180)	P7 - ΣK_p	P6 - ΣK_p	P6 - P7
Delay (days)	27	180	+4	-10	-14
s.d. in Units of ΣK_p	8.4	11.0	10.5	11.9	9.7

The first quantity in Table 4 indicates that the 27-day recurrence tendency was not particularly strong in 1968, because the standard deviation of Pioneer VII measurements from those obtained 27 days later was 8.4 (in units of ΣK_p) whereas the random errors of measurement appeared from the data to be only one or two units. Standard deviations of Pioneer VII measurements six months apart were also calculated, yielding an s.d. of 11, which should correspond to uncorrelated data. The s.d.'s between a series of measurements, a_i, and another series, b_i, were calculated by the formula

$$\text{s.d.} = \sqrt{\frac{\sum_N (a_i - b_i)^2}{N}}$$

When Pioneer VII measurements were used to predict the measurements of Pioneer VI two weeks later, the s.d. was larger than that of a 27-day prediction of Pioneer VII by itself. This suggests the influence of biases or nonlinearities in the measurements, although temporal or spatial fluctuations in the solar wind could be responsible. When Pioneer VII data alone were co-rotated to provide a simple prediction of ΣK_p, the error was nearly as large as six-month predictions of Pioneer VII, suggesting that the complications introduced by the penetration of the magnetosphere were at least sufficient to increase the s.d. from 8.4 to 10.5; i.e., nearly sufficient to cause the predictions to be uncorrelated with the quantity being predicted. When Pioneer VII data were used to predict ΣK_p, the two appeared to be uncorrelated. In fact, it would appear from these data that any prediction with an s.d. above about 10 units is uncorrelated with the quantity being predicted.

Having established this basic information about the data, we proceed to a statistical evaluation of the predictions of ΣK_p. Table 5 lists the s.d.'s of predictions by several methods:

TABLE 5

STANDARD DEVIATIONS OF PREDICTIONS OF ΣK_p

Quantities	Prediction of Fig. 11	$\Sigma K_p - \overline{\Sigma K_p}$	$\Sigma K_p(t) - \Sigma K_p(t-2)$	$P7 - \Sigma K_p$
s.d. in Units of ΣK_p	10.8	8.6	10.8	10.5

The predictions using the co-rotated solar wind speed from Pioneer VII and the flare-associated precursors, which is illustrated in Figure 11, is not significantly better than a value picked at random. We attribute this negative result to the fact that riometers are insensitive to the smaller PCA's, and some of the other precursors are available only part of the time. We expect that this result would be improved if data from polar ionosondes and other sensitive measurement methods were available for 1968 on a 24-hour basis.

A prediction, using the annual average, is (surprisingly) the best of the four methods compared in Table 5. This number was arrived at independently by two different computers, so it is correct. It corresponds to an error of 1.1 units in the predicted value of K_p. The predictions based on two-day persistence and the Pioneer VII solar wind speed are not significantly different from that of Figure 11, or from a random guess.

The conclusions to be deduced from this statistical analysis are that the annual average is, at the present time, better than any of the more sophisticated methods of predicting K_p employed in this report. More research on the flare-associated events is obviously needed. This research should be directed toward the more sensitive methods, such as ionosondes in polar locations, and toward obtaining complete 24-hour coverage of the flare-associated precursors.

3.4 SUGGESTIONS FOR FUTURE RESEARCH

There are two lines along which future research could profitably be conducted: One is to study the usefulness of additional precursors in the prediction of flare-associated magnetic storms. Some of the best precursors are not yet available for the year 1968, but will later become available. These will be discussed in Section 3.4.1. The second future research area is the instrumentation and evaluation of a space probe which is specifically designed to aid in the prediction of geomagnetic storms. The orbit and instruments which would be desirable for such a research project will be briefly discussed in Section 3.4.2.

3.4.1 Further Studies Involving Precursors

Although many precursors have been utilized in the present study, some of the precursors used had gaps in geographical or temporal coverage. For example, we only have data on solar radio noise bursts from North America, and the solar x-ray data appear not to cover all times. Other promising precursors are not yet available for the year 1968. Among the unavailable data are polar ionosonde, HF oblique-incidence, polar airglow, and prompt energetic electron measurements. A search for small PCA's would be desirable, using polar ionosonde (Reference 26) and HF oblique-incidence measurements (References 24, 25) for 1968 (when they become available).

To facilitate future research, and for the improvement of the storm-predicting networks, it would be desirable that each high-latitude riometer have an ionosonde near it, and that the ionosonde measurements be reduced immediately. (There is an ionosonde four miles from the riometer at McMurdo Sound, Antarctica, but the ionosonde measurements do not become available for several years after they are recorded.) The differences in absorption between day and night, which were studied by Adams and Masley (Reference 27), should be studied for diagnostic value, because the energy spectrum of energetic solar particles might affect radio propagation and magnetic storms in different ways. The sector structure and the southward pointing field component may affect the interaction between solar plasma and the magnetosphere, so this effect should be looked for when these data become available for 1968. Correlated studies for 1968, using long distance HF radio propagation (References 24, 25) and VLF phase anomalies (Reference 28), could be quite informative, especially if the energy spectrum revealed by diurnal variations observed with polar riometers were taken into account.

Some additional precursors have been reported in recent years; Castelli and Arons have reported that the spectrum of solar radio noise bursts can be used to predict geomagnetic storms (Reference 29). Adkinson and Hoffman have reported that half of the magnetic storms which occurred between April, 1965, and May, 1966,were preceded by a peculiar transient seen in the geomagnetic records at middle latitudes (Reference 30).

Mathews et al. (Reference 31) have used super neutron monitor data at many low-latitude stations around the world to study the anisotropy of Forbush decreases and "pre-decreases." The "pre-decrease" may be the result of the turbulent plasma cloud or shock front scattering cosmic rays away from the earth. These "pre-decreases" are sometimes seen at certain low-latitude stations before a storm's sudden commencement. Their possible predictive value should be investigated when the measurements for 1968 become available. When data on these new precursors become available for 1968, they should be compared with the other data for the same year.

Because so many kinds of data are involved, it appears that a cooperative study would be required to evaluate all the precursors and their interrelations. The MDAC Space Sciences Department would gladly contribute its polar riometer data, as well as the graphs of many precursors during 1968. Although there was little 27-day recurrence tendency in the data for 1968, this is not too surprising, because recurrence becomes more prominent later in the sunspot cycle. There will be an opportunity to study recurrence in the 1970 - 1975 data when that time comes. A satellite in the Vela orbit would be desirable, in addition to at least two Pioneer space probes, but the present velocity resolution of Vela solar wind data is too coarse to be of much use. Also, data from the Pioneers and Vela should be made available at more frequent intervals than the three or four samples per day which are being published in 1969. (In 1968, only one measurement per day was published). Finer time resolution would be helpful in evaluating the correlation between geomagnetic storms and changes in the solar wind speed, which has been reported by Venkatesan and Sreenivasan (Reference 32).

One other possibility which should be investigated in a future study is the direct prediction of A_p from the precursors when the predicted $\Sigma K_p > 50$. This is desirable because it can be seen from Figure 4 that the corpuscular energy input is nearly proportional to A_p when $K_p > 6$ ($\Sigma K_p > 48$), while it is proportional to K_p when $K_p < 6$. Direct predictions of A_p could not be investigated in the present study because K_p only reached 50 on two occasions in 1968. In the next several years, as K_p reaches its solar-cycle peak, there will be a number of days for which direct predictions can be made and studied.

3.4.2 A Space Probe for Use in Predicting K_p

The orbit occupied by the Pioneer VII Space Probe, which is illustrated in Figure 6, is ideal for sampling the long-lived solar streams which will be passing over the earth three days later. The measurements of solar-wind speed made by this type of spacecraft will be useful for predicting the recurring geomagnetic storms. This type of storm is not so common during periods of rising solar activity, but it becomes very prominent during the declining part of the solar cycle.

For detecting the solar x-rays, UV radiation and energetic particles that are produced by the major solar flares which often precede geomagnetic storms, it would be desirable for the space probe to be able to scan the sun at one or several UV or x-ray wavelengths. Such a scanning system has been flown on OSO-4, but a less elaborate system would be satisfactory for predicting magnetic storms. The knowledge gained from the Harvard College Observatory experiment aboard OSO-4 will be helpful in designing a prediction system. In this connection, Dr. George Withbroe or Dr. Leo Goldberg could be contacted at the Harvard College Observatory, 60 Garden Street, Cambridge, Massachusetts.

The reason that it is important to scan the sun, rather than merely measuring the total solar emission,is that the response at the earth depends strongly on the location of the solar flare. In data presently available, it is sometimes impossible to determine the location of the flare which produced the UV and particulate emissions.

Section 4

LONG-TERM PREDICTIONS OF THE ANNUAL AVERAGE OF A_p

In this section, we attempt to predict the annual average value of A_p until the year 2030. The first step is to predict the sunspot cycle, because sunspot records date back several centuries, allowing their periodicities to be known. King-Hele (Reference 33) and Xanthakis (Reference 34) have made predictions of future sunspot cycles. The theoretical foundations of the predictions are questionable, but it is necessary to have predictions, so these were used. An average prediction based on material in References 33 and 34, with some additional material from Waldmeier (Reference 35), is given in Figure 12. The predicted annual average Zurich Relative Sunspot Number, $\overline{R_z}$ is shown for each year from 1968 to 2030. $\overline{R_z}$ is given in tabular form in Table 6.

The method of predicting $\overline{A_p}$, the annual average of A_p, using the sunspot cycle, is based on the work of Gnevyshev (Reference 19). Gnevyshev has shown that several of the measures of solar activity are closely correlated with $\overline{A_p}$, if measurements are restricted to the part of the sun within $\pm$ 30° of the earth-sun line. Gnevyshev's comparison between $\overline{A_p}$ and the coronal green line is shown in Figure 13. His curve of the sunspot area in 5° latitude intervals is shown in Figure 14. In both cases, the correlation with $\overline{A_p}$ is obvious. To find the specific relationship between $\overline{A_p}$ and $\overline{R_z}$, these quantities are plotted for the three sunspot cycles, 1937 - 1968 in Figure 15. The data from these three cycles have then been averaged to obtain Figure 16. Using information gained from Figures 12 through 16, values of $\overline{A_p}$ to the year 2030 have been predicted and plotted in Figure 17. The predicted values of $\overline{A_p}$ are also given in Table 6, along with the predicted sunspot numbers.

It is difficult to estimate the standard deviations (s.d.) which should be assigned to these predictions of $\overline{A_p}$ and $\overline{R_z}$. Judging by the correlations and scatter among the data from past measurements presented in this section, we would assign an s.d. of 10% to predictions of $\overline{A_p}$ and $\overline{R_z}$ for the remainder of

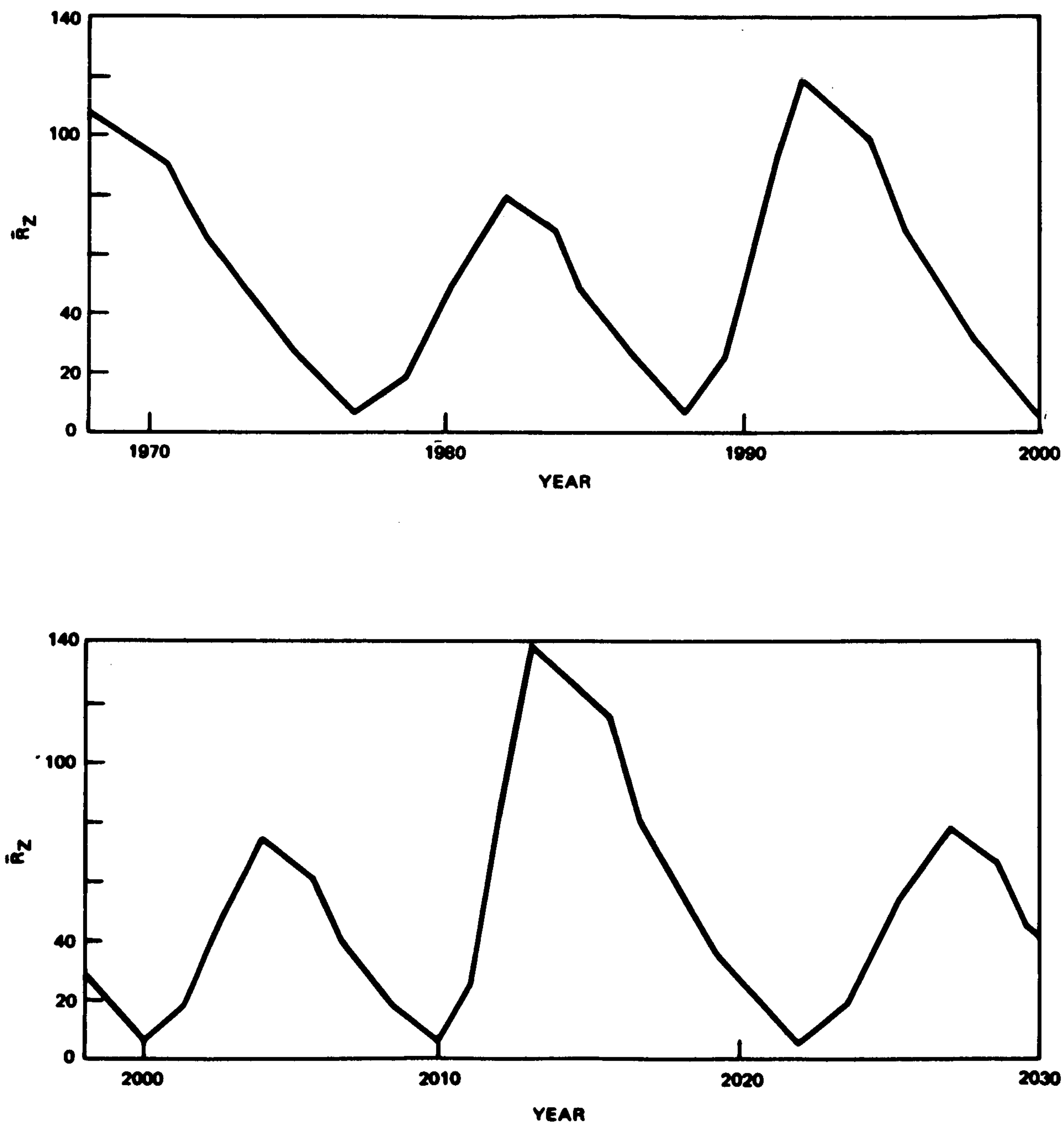

Figure 12. Predicted Annual Average Zurich Relative Sunspot Number, $\overline{R_Z}$

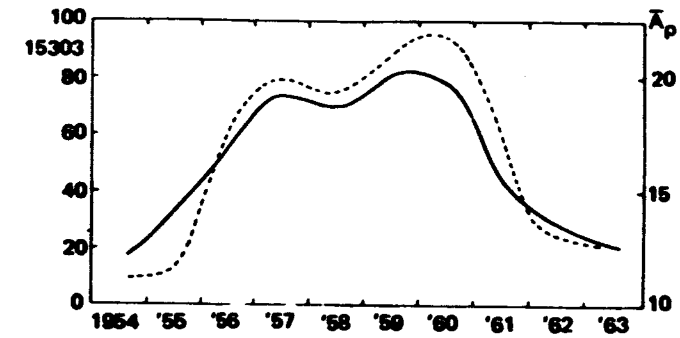

Figure 13. The Variation of the Geomagnetic Index Ap and of the Coronal Line Intensity at 5303A Averaged Over ± 30° from the Direction to the Earth (After Gnevyshev)

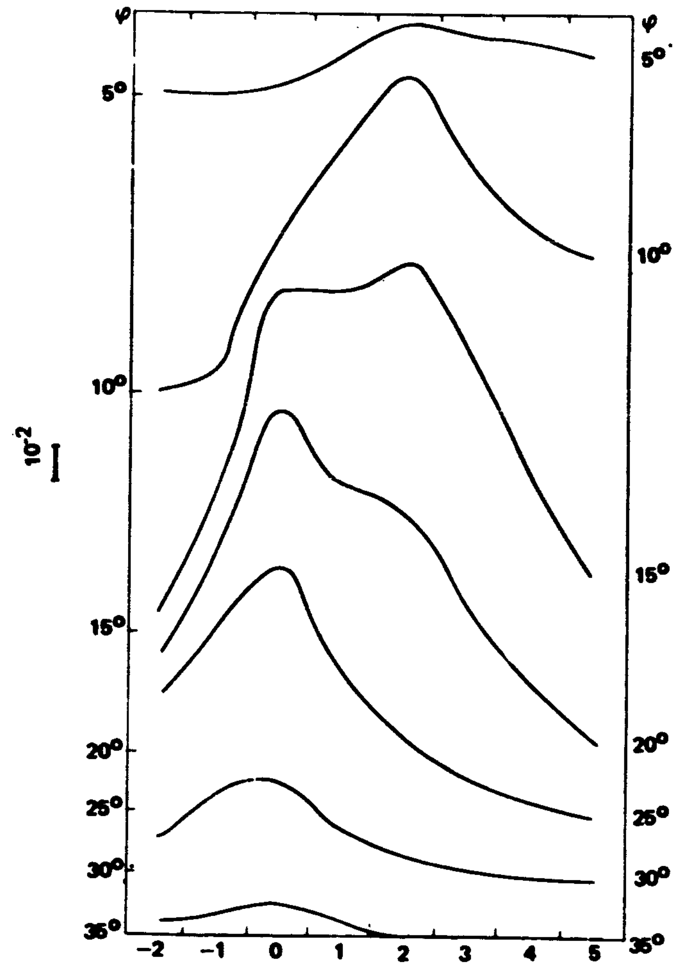

Figure 14. Variation of the Sunspot Area in Latitude Intervals of 5° Wide during the 11-Years Cycle (After Gnevyshev)

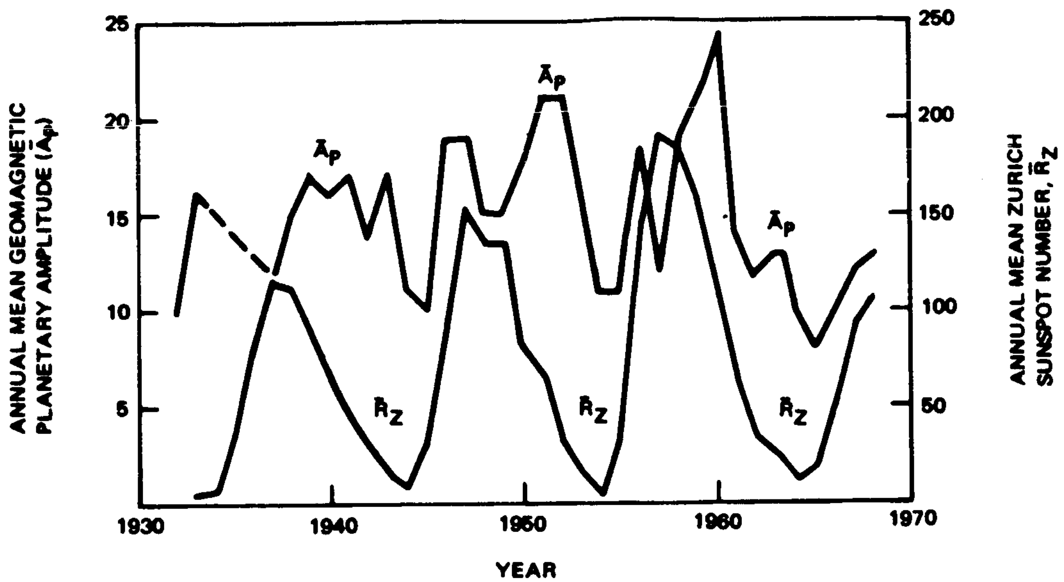

Figure 15. Comparison of $\bar{A}_p$ and $\bar{R}_Z$ from 1932 to 1968

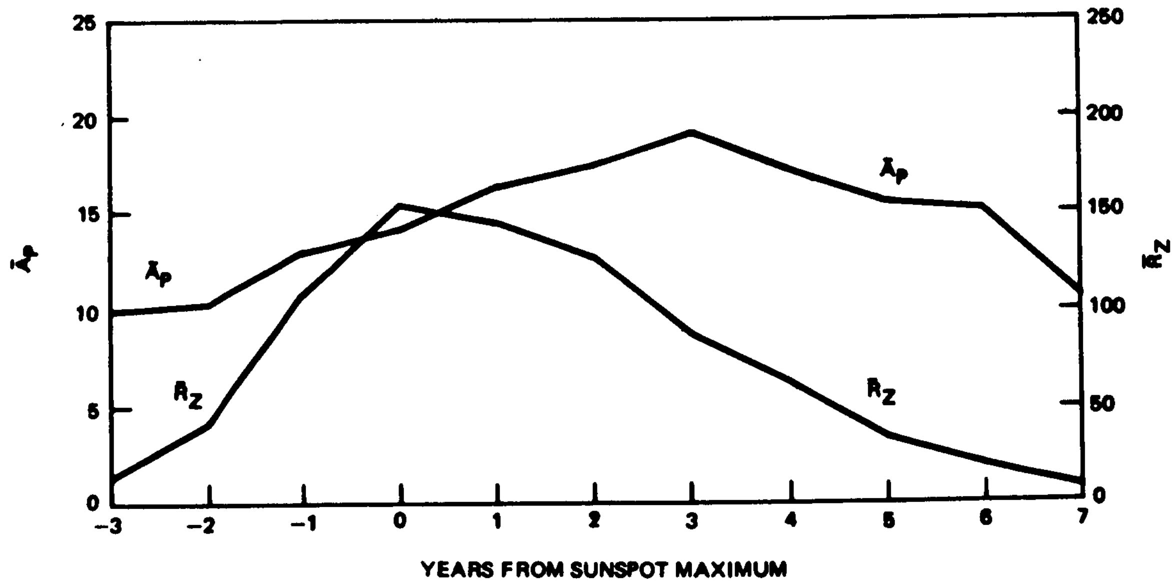

Figure 16. Average Dependence of $\bar{A}_p$ and $\bar{R}_Z$ on Time from Sunspot Maximum

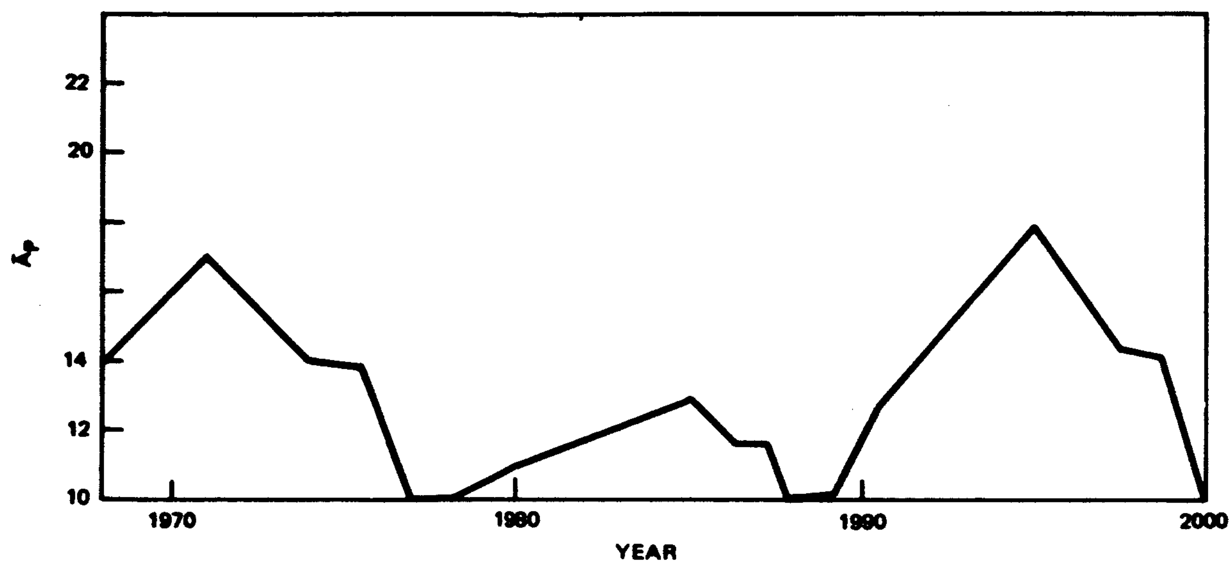

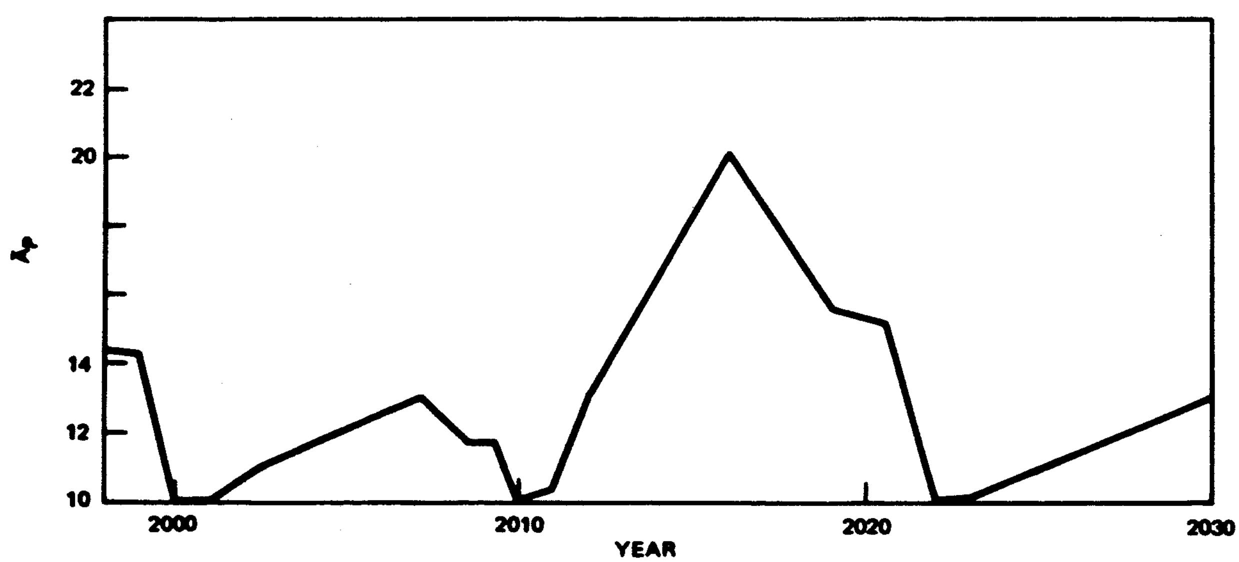

Figure 17. Predicted Annual Average Geomagnetic Planetary Amplitude, $\bar{A}p$

TABLE 6

PREDICTED ANNUAL AVERAGES OF SUNSPOT NUMBER, $\overline{R_Z}$,

AND GEOMAGNETIC PLANETARY AMPLITUDE, $\overline{Ap}$

Date	$\overline{R_z}$	$\overline{Ap}$	Date	$\overline{R_z}$	$\overline{Ap}$
1968	107	14	2000	7	10
1969	101	15	2001	14	10
1970	94	16	2002	33	11
1971	83	17	2003	55	11
1972	64	16	2004	75	12
1973	51	15	2005	67	12
1974	38	14	2006	56	13
1975	26	14	2007	38	13
1976	16	13	2008	25	12
1977	7	10	2009	15	12
1978	14	10	2010	7	10
1979	27	10	2011	27	10
1980	47	11	2012	87	13
1981	64	11	2013	140	15
1982	80	12	2014	132	16
1983	73	12	2015	122	18
1984	61	13	2016	103	20
1985	42	13	2017	78	19
1986	30	12	2018	60	17
1987	18	12	2019	41	16
1988	7	10	2020	28	15
1989	20	10	2021	17	14
1990	50	12	2022	7	10
1991	87	13	2023	14	10
1992	120	14	2024	27	10
1993	110	16	2025	47	11
1994	102	17	2026	64	11
1995	82	18	2027	80	12
1996	60	16	2028	73	12
1997	43	15	2029	61	13
1998	29	14	2030	42	13
1999	16	13			

the present sunspot cycle, 20% for the next cycle, and 25% for subsequent cycles.

Section 5

CONCLUSIONS

A new method of making short-term predictions of K_p and A_p has been developed and tested, using the available solar and geophysical data for 1968. The method employs Pioneer VII measurements of the solar wind speed as basic data. An attempt is made to separate the contributions to K_p from recurrent storms and from flare-associated storms by using various storm precursor data. This first test of the method failed to produce the hoped for improvement, but did not disprove the method because the flare-associated precursors did not cover the full 24-hour day, and only one ten-minute sample of the solar wind speed was available each day. A further test of the method would be desirable when complete data becomes available. A number of suggestions for further research are made in this report.

Long-term predictions of the annual average of K_p and the Zurich relative sunspot number have also been developed in the present report. These predictions are based on earlier work by Gnevyshev, King-Hele and Xanthakis. Predicted values for each year until 2030 are presented in graphical and tabular form. These long-term predictions should satisfy the needs of the Marshall Space Flight Center for mission planning.

REFERENCES

1. Bartels, J., "Geomagnetic Indices," Ann. de Geophysique, 1963.

2. Moe, K., and D. Nebergall, "Variation of Geomagnetic Disturbance With Latitude," J. Geophys. Res. 74, 1305-7, March 1, 1969.

3. Moe, K., On the Inadequacy of Present Global Atmospheric Models and Deductions Based on Them, invited paper presented at 12th COSPAR Meeting, Prague, 1969 (MDAC Paper No. 10,127).

4. Moe, K., Planet. Space Sci., 15, 1821 (1967).

5. Jacchia, L. G., Smithsonian Astrophys. Obs. Sp. Rept. No. 150 (1963).

6. Small, H. W., "Atmospheric Density Between 70 and 200 Nautical Miles from Satellite Observations," Lockheed Missiles and Space Co., A376332, (1964).

7. Jacobs, R. L., J. Geophys. Res., 72, 1571 (1967).

8. Truttse, Yu. L., Planet. Space Sci., 17, 181 (1969).

9. Dessler, A. J., J. Geophys. Res., 64, 397 (1959).

10. Cole, K. D., Australian J. Phys., 15, 223 (1962).

11. Campbell, W. H., J. Geophys. Res., 72, 3429 (1967).

12. Georges, T. M., J. Atmos. Terr. Phys., 30, 735 (1968).

13. Hines, C. O., J. Geophys. Res., 70, 177 (1965).

14. Wescott, E. M., J. D. Stolarik, and J. P. Heppner, "Electric Fields in Auroral Forms," X-612-69-22, Goddard Space Flight Center (1969).

15. DeVries, L. L., E. W. Friday, and L. C. Jones, Space Research VII, ed. by R. L. Smith-Rose, S. A. Bowhill, and J. W. King, p. 1173, North-Holland Publ. Co., Amsterdam (1967).

16. Snyder, C. W., M. Neugebauer and U. R. Rao, "The Solar Wind and its Correlation with Cosmic-Ray Variations and with Solar and Geomagnetic Activity," J. Geophys. Res., Vol. 68, pp. 6361-6370,(1963).

17. Moe, K.,"A Study of the Reliability of PCA as a Predictor of Geomagnetic Storms," J. Geomag. Geoelectr., 18, 159-66, (1966).

18. Ballif, J. R., D. E. Jones, P. J. Coleman, Jr., L. Davis, Jr., and E. J. Smith, J. Geophys. Res., Vol. 72, pp. 4357-64.

19. Gnevyshev, M. N., Solar Physics, 1, 107-120, (1967).

20. Solar-Geophysical Data, ESSA (monthly).

21. Ballif, J. R., D. E. Jones, P. J. Coleman, Jr., L. Davis, Jr., and E. J. Smith,"Further Evidence on Correlation," J. Geophys. Res., (in press).

22. Anderson, K., Unpublished data.

23. Akasofu, S-I., and S. Yoshida, "The Structure of the Solar Plasma Flow Generated by Solar Flares," Planet Space Science, Vol. 15, pp. 39-47, (1967).

24. Jelly, D. H., J. Geophys. Res., 68, 1705, (1963).

25. Hakura, Y., and J. V. Lincoln, J. Geophys. Res., 68, 1563, (1963).

26. Jelly, D. H., and C. Collins, Canadian J. Phys., 40, 706, (1962).

27. Adams, G. W., and A. J. Masley, Planet. Space Sci., Vol. 14, pp. 277-290, (1966), (Douglas Paper No. 3112).

28. Chilton, C. J., F. K. Steele and R. B. Norton,"VLF Phase Observations," J. Geophys. Res., Vol. 68, pp. 5421-35, (1963).

29. Castelli, J. P., J. Arons and G. A. Michael, "Flux Density Measurements of Radio Bursts," J. Geophys. Res., Vol. 72, pp. 5491-8, (1967).

30. Adkinson and Hoffman, "Abstract of Paper ST53," Trans. AGU, Vol. 49, p. 728, (1968).

31. Mathews, T., J. B. Mercer and D. Venkatesan, Anistropy in Cosmic Ray Intensity, The University of Calgary, (1967).

32. D. Venkatesan and S. R. Sreeninasan, The Solar Wind and the Significance of ΣK_p, University of Calgary, (1967).

33. King-Hele, D. G., "Prediction of Sunspot Maxima," Nature, Vol. 209, pp. 285-6, (1966).

34. Xanthakis, John, "Time of Rise of Sunspot Cycles," Nature, Vol. 215, pp. 1046-8, (1967).

35. Waldmeier, M., Sunspot Activity in the Years 1610-1960, Schultheis and Co., Zurich, (1961).